Transport of granular matter on an inclined vibratory conveyor with circular driving

Hamid El hor

Department of Physics, Jazan University, KSA

Abstract— *I present a theoretical model to investigate the transport properties of granular materials on an inclined vibratory conveyor driven by circular oscillations. My model treats the granular dynamics on a vibratory conveyor as a combination of sliding and oblique hopping of a granular block with specific inelastic and frictional properties. The calculations show optimal transport conditions for the transport velocity efficiency, with an extra transport velocity efficiency minimum when the inclination of the vibratory conveyor is non zero. The investigations also show a current reversal under a certain inclination angle which does depend on the friction force.*

Keywords— Granular matter, vibratory conveyors, transport velocity efficiency, current reversal, optimal transport conditions.

I. INTRODUCTION

Vibratory conveyors, i.e., troughs that induce the motion of the material laying on them when they are oscillating, are extensively used in industry for the handling and transport of granular materials. They present many advantages such as the simplicity of their construction, the controllable feeding speed, the possibility of mixing and/or segregating different types of granular materials laying on them by tuning the right oscillating frequencies, and finally the self-cleaning operating

mode [1–4]. Consequently, extensive theoretical and experimental [3–15] studies were devoted to the properties and dynamic of granular materials on these devices using mainly two types of driving modes: linear and circular. The experimental investigations revealed the existence of optimal transport conditions, i.e., maximal and minimal transport velocity for special throw numbers $\Gamma=a_{max}/g\cos(\alpha)$, where a_{max} is the maximal vertical acceleration, α the trough inclination angle, and g is the gravitational acceleration. Moreover, the transport velocity of granular materials using a circular driving mode showed a surprising current reversal as a consequence of a continuous variation of Γ. Previous theoretical investigations using macro-mechanical models for the hopping and gliding dynamics reproduced successfully the experimental findings [3, 11, 12], and explained the dynamical origin of the optimal transport conditions.

In this work, I investigate the effect of the tilt of a vibratory conveyor driven by circular oscillations on the transport properties of granular materials. More specifically, I investigate the effects of this tilt on the current reversal and on the optimal transport dynamics.

II. MODEL

The basic setup of an inclined vibratory conveyor is schematically sketched in Fig.1. The angle α represents the inclination of the trough relative to the horizontal. The frame XOY is fixed in space, whereas the frame *xoy* is attached to the trough and is co-moving with it. The positive transport direction as shown in the figure, is upward. The trough is driven by circular oscillations:

$$X = A\cos(\omega t) \quad (1)$$

$$Y = A\sin(\omega t) \quad (2)$$

Where t is the time, X and Y are the coordinates of the troughin the XOY frame, A the amplitude of the trough oscillations, and ω the oscillation frequency of the conveyor.

The model is based on the assumption that the motion of the moving granular material is that of a granular block with constant mass m. It also assumes that the granular block can perform two distinct types of dynamics: sliding and bouncing motions under the action of the driving forces. We also suppose that collisions between the granular block and the trough after oblique hopping are instantaneous and, by inference, generally inelastic.

The transition from sliding to hopping happens as soon as the following lift–off condition is fulfilled:

$$\omega^2 A\sin(\omega t) - g\cos(\alpha) > 0, \tag{3}$$

where g is the gravitational constant. As long as the projected gravitational acceleration gcos(α) is larger than the conveyor driving acceleration in the Y–axis, the granular block will perform a gliding motion (G–phase). If equation(3) is fulfilled, the granular block will detach from the trough and start a free flight phase (F–phase). In the following, the dynamics of these two phases and the transitions between them are discussed in detail.

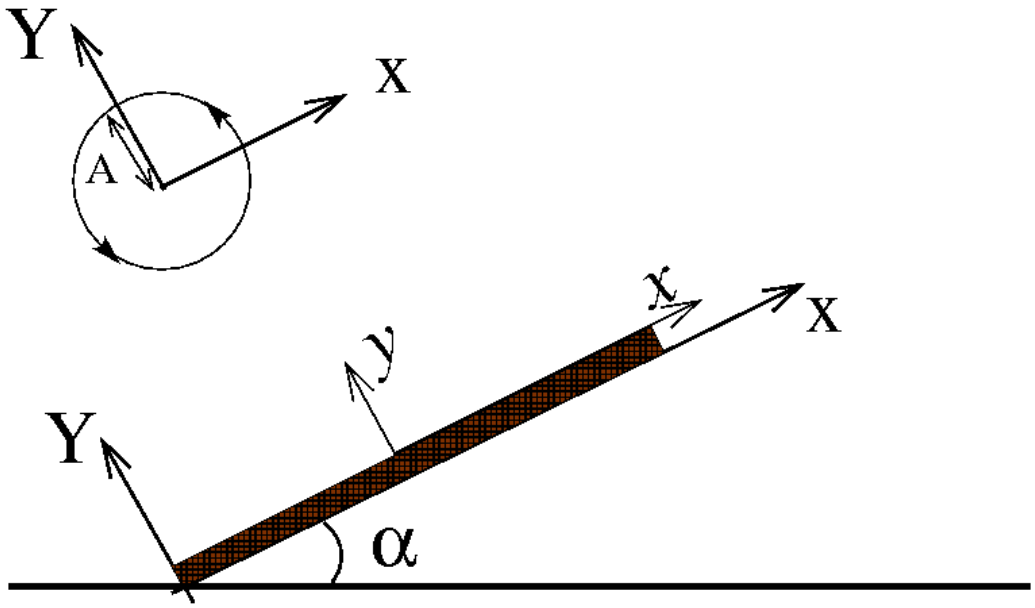

FIG. 1: The basic setup of the inclined vibratory conveyor. α is the inclination angle. The frame xoy is co–moving with the trough, while XOY is fixed in space.

1.1 Gliding phase

A gliding phase takes place if, after the granular block hits the trough, the lift–off condition (3) is not fulfilled. During this phase the granular block performs a sliding motion subject to gravitation and friction forces. The corresponding equations of motion in the co–moving frame are determined by:

$$m\ddot{x} = \omega^2 mA\cos(\omega t) - g\sin(\alpha) + F \tag{4}$$

$$m\ddot{y} = \omega^2 mA\sin(\omega t) + N - mg\cos(\alpha) \tag{5}$$

Where F is the friction force acting on the block. The problem of the granular friction is an open and complex problem [16, 17] with many intervening parameters such as the size and shape of the particles, as well as the particle and the container wall roughness. In this work, and for the sake of simplicity, we use the solid coulomb like friction F_{solid} as friction force [3, 4, 8] which is defined by:

$$F_{solid} = \mu sgn(\dot{x})N \tag{6}$$

here, the dynamic friction coefficient μ is not directly related to the frictional behavior of a single grain. It rather comprises the whole complexity of the sliding behavior of the underlying interacting many-grain system. Furthermore, N denotes the normal reaction force which is determined in this case by:

$$N = -m\omega^2 A\sin(\omega t) + mg\cos(\alpha) \tag{7}$$

Inserting (6) and (7) into (4) yields:

$$\ddot{x} = \omega^2 A\cos(\omega t) - g\sin(\alpha) - \mu sgn(\dot{x})(g\cos(\alpha) - \omega^2 A\sin(\omega t)) \tag{8}$$

The solution for the horizontal velocity resulting from (8) reads:

$$\dot{x} = \omega A\,(\sin(\omega t) - \sin(\omega t_0)) - g\sin(\alpha)(t - t_0) - \mu sgn(\dot{x})[g\cos(\alpha)(t - t_0) + \omega A(\cos(\omega t) - \cos(\omega t_0))] + \dot{x}_0 \tag{9}$$

The index 0 denotes the initial condition at the impact and the start of the gliding phase. If the velocity changes its sign, the index 0 indicates that the solution of (8) must be reiterated with the initial condition at the time of this change. During a gliding phase, the position and the velocity of the granular block in the y–direction obviously equals zero.

1.2 Free flight phase

The free flight phase starts once the condition in (3) is fulfilled. The lift–off time t_l is determined by the condition:

$\omega^2 A\sin(\omega t) g\cos(\alpha) = 0$. The equations of motion in the co–moving frame are then given by:

$$m\ddot{x} = m\omega^2 A\cos(\omega t) - mg\sin(\alpha) \tag{10}$$

$$m\ddot{y} = m\omega^2 A\sin(\omega t) - mg\cos(\alpha) \tag{11}$$

Using the lift–off initial conditions, namely $x(t_l) = x_l$, $y(t_l) = 0$, $\dot{x}(t_l) = \dot{x}_l$, $\dot{y}(t_l) = 0$, we obtain:

$$\dot{x} = \omega A(\sin(\omega t) - \sin(\omega t_l)) - g\sin(\alpha)(t - t_l) + \dot{x}_l \tag{12}$$

$$\dot{y} = -\omega A(\cos(\omega t) - \cos(\omega t_l)) - g\cos(\alpha)(t - t_l) + \dot{y}_l \tag{13}$$

The subsequent impact time is determined by the next zero of the solution of the equation for y(t) with the afore-mentioned initial conditions for the lift–off.

1.3 Collisions with the trough

Collisions between the granular block and the trough are generally inelastic. The velocity of the granular block after the collision is given by:

$$\dot{x}_i = \varepsilon_t \dot{x}(t_i) \tag{14}$$

$$\dot{y}_i = -\varepsilon_n \dot{y}(t_i) \tag{15}$$

where the subscript i reflects the corresponding values right at the impact. The restitution coefficients ε_t and ε_n can take arbitrary values from 0 to 1. A step–by–step iteration of the combination of these dynamical phases determines the dynamics of the granular block in an algorithmic way.

III. RESULTS AND DISCUSSION

The equations of the previous section are numerically solved and the different dynamic phases as well as the transport velocity are calculated. We define the transport velocity as the mean value of finite velocities of the granular block along the trough obtained during the different dynamic phases for several conveying cycles (with the period $T = 2\pi/\omega$). We also introduce the dimensionless transport velocity efficiency [8] which is defined as the ratio of the granular block velocity and the maximum tangential trough velocity: $\eta = \langle V \rangle / A\omega$. We assume in this work that due to the internal interactions between the particles, the granular block looses all its normal velocity when it hits the trough (soft cheese approximation), hence we set the normal restitution coefficient to zero ($\varepsilon_n = 0$). While, due to the flow, the tangential restitution coefficient is non zero ($\varepsilon_t \neq 0$). We also fix the driving amplitude to the dimensionless arbitrary value A = 0.01, leaving us with three free parameters: the friction coefficient μ, the tangential restitution coefficient ε_t and the inclination angle α. We present in Fig.2 the transport velocity efficiency η of the granular block as function of the dimensionless throw number $\Gamma = A\omega^2/g\cos(\alpha)$, calculated for $\alpha = 0°$ using $\mu = 0.3$, for $\alpha = 10°$ using $\mu = 0.3$ and $\mu = 0.6$ and finally, for $\alpha = 30°$ using $\mu = 0.6$. The tangential restitution coefficient was set to $\varepsilon_t = 0.7$ for all these calculations. The figure shows many similarities between the velocity efficiency calculated for $\alpha = 0$ and $\alpha = 10°$. The results show, at both inclination angles, the existence of a critical value $\Gamma_c(\alpha, \mu)$ below which the velocity efficiency is zero. The calculations show that this critical throw number depends on the inclination angle α as well as on the friction coefficient μ. By increasing the acceleration above this threshold a non zero transport velocity efficiency is obtained which is non monotonous and has optimal transport conditions with two maximums at $\Gamma \approx 1.2$ and $\Gamma = 4.7$ and a minimum at $\Gamma = 3.7$. The first maximum is however more pronounced for $\alpha = 10°$ when we use a smaller friction coefficient $\mu = 0.3$. A higher friction coefficient smears the velocity efficiency out at and around this maximum. Fig.2 shows a second velocity efficiency minimum for $\alpha = 10°$ at $\Gamma \approx 0.6$ which lays at $\Gamma < 1$ where only sliding motion is possible. Since the dynamics of the granular block at this minimum are those of a sliding motion (G-phase), its position depends on the friction force as also shown in Fig. 2 (the position of this minimum differs when we use $\mu = 0.3$ and

μ = 0.6). For larger throw numbers, the positive driving acceleration becomes large enough to weaken the downhill flow leading to an increase in the flow velocity.

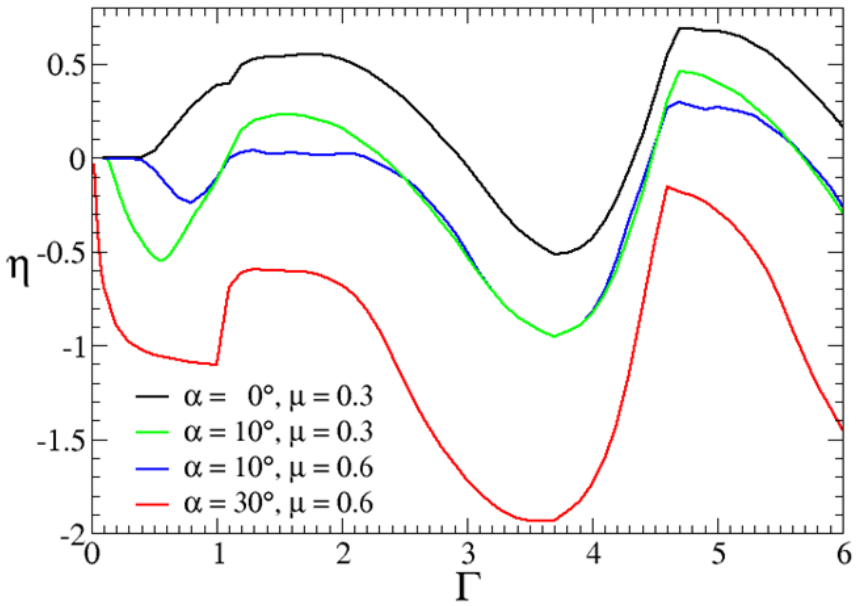

FIG. 2: The transport velocity efficiency η = hν/Aωi as function of the throw number Γ = Aω 2 /gcos (α) calculated using ε_t = 0.7 and μ = 0.3 for α = 0 (black) and α = 10° (green). The velocity efficiency (in blue and red) is calculated using the same tangential restitution coefficient ε_t = 0.7 while the friction coefficient was set to μ = 0.6 for α = 10° and α = 30° respectively.

We also see in Fig. 2 that the transport velocity efficiency for α = 0 and α = 10° oscillates between negative and positive values of velocity efficiency and subsequently reversing the transport direction many times. Such behavior is called transport current reversal. Extensive calculations proved that these properties, i.e., optimal transport conditions and current reversal, are robust under parameter variations (restitution coefficient ε_t , friction coefficient μ, and driving amplitude A) as far as we do not use unphysical high values for the friction coefficient μ.

Our calculations allow us to plot an individual solution which gives us some insight into the global dynamics of the granular block. To describe qualitatively the motion of the granular block, we plot in Fig.3 the bifurcation diagram which shows the relative F–phase time τ as function of the throw number Γ. The relative $_{\text{F–phase time } \tau = t}$F/T is defined as the Fig. 3.
Fig. 3.

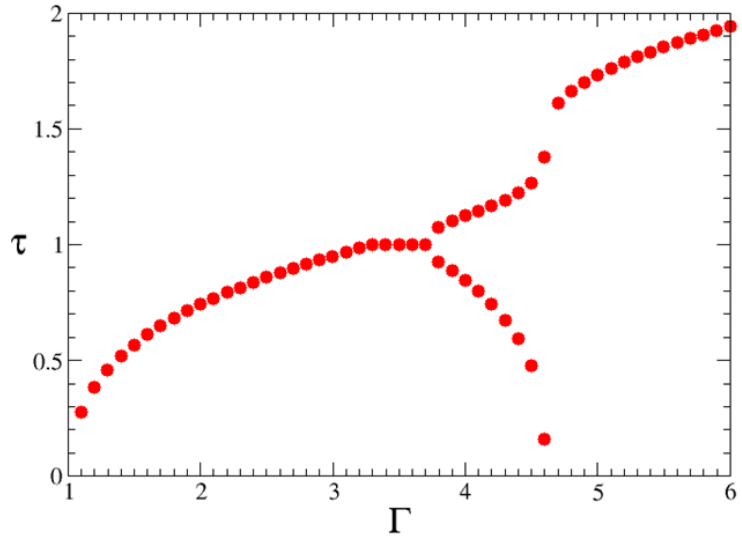

FIG. 3: Bifurcation diagram: the time of flight τ , which is the time of a free flight phase, as function of the throw number Γ = Aω^2 /gcos(α) calculated for an inclination angle α = 20° and using a driving amplitude A = 0.01, a solid friction coefficient μ = 0.3 and a tangential restitution coefficient ε_t = 0.6, while the normal restitution coefficient was set to ε_n = 0.

The figure shows a bifurcation point at $\Gamma = 3.7$ fraction of the free flight time t_F, the time of a free flight phase, to the period of the driving oscillations $T = 2\pi/\omega$. For $\Gamma \leq 1$ the lift–off condition in (3) cannot be fulfilled, hence the granular block is permanently in contact with the trough. The dynamics are reduced in this case to those of a gliding phase and we have $\tau = 0$. As the throw number departs from $\Gamma = 1$, the Y component of the conveyor acceleration becomes larger than the gravitational component $g\cos(\alpha)$ at some phases of the driving cycle. Under these conditions, the lift–off condition is fulfilled and hence, the granular block can perform a free flight motion. The duration t_F of the free flight phase increases progressively as the acceleration increases. Subsequently, the relative free flight time departs from zero and increases proportionally to the throw number Γ as shown in Fig.3.

In the range $(1 < \Gamma < 3.3)$, the motion of the granular block is periodic with a single period composed of one gliding phase followed by a free flight phase. This is where the first maximum takes place. Fig.5, which plots the time evolution of the position of the granular block in the Y direction, shows that the beginning of the gliding phase and that of the positive phase of the driving acceleration cycle coincides at the maximum. The free flight time t_F keeps increasing as the driving acceleration increases until it is equal to the driving oscillations period T , which takes place at $\Gamma = 3.3$ and persists until

$\Gamma = 3.7$. Here the motion of the granular block consists of hopping without gliding. The minimum transport velocity of the granular block takes place at $\Gamma = 3.7$. The dynamics of the granular block at this minimum are those of a free flight phase and, subsequently, are independent of friction.

The bifurcation point in Fig.3 coincides with the minimum transport velocity $\Gamma = 3.7$. For $3.7 \leq \Gamma < 4.7$ we obtain two solutions for the equations of motion of the granular block. These two solutions correspond to two different free flight phases, one with $\tau_1 < 1$ and decreasing as the driving acceleration increases until it vanishes at $\Gamma \approx 4.7$. The second free flight phase has a free flight time larger than the driving period ($\tau_2 > 1$) which keeps increasing as the driving acceleration increases. The total free flight time $\tau = \tau_1 + \tau_2$ decreases as far as we have two solutions. As the throw number increases, the beginning of the gliding phase moves from the negative phase of the driving cycle to the positive one, which leads to an increase of the transport velocity efficiency in the range $3.7 \leq \Gamma \leq 4.7$. Finally, the second maximum velocity efficiency is at $\Gamma \approx 4.7$ where the beginning of the gliding phase coincides with that of the positive acceleration phase of the driving cycle as it is the case for the first maximum, but here with a period doubling as shown in Fig. 5.

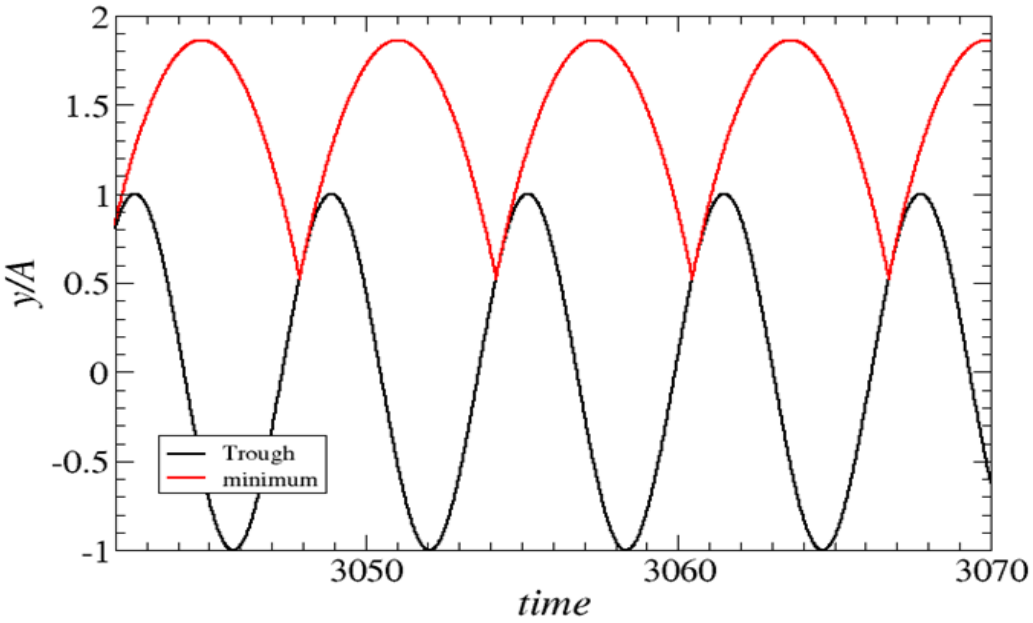

FIG. 4: The vertical motion of the granular block (red solid line) and of the table (black solid line) at minimal transport velocity $\Gamma = 3.7$ as function of time. At the minimum the motion of the granular block is periodic and consists on successive and similar free flight phases.

One can conclude that as far as the driving acceleration is large enough, we obtain a maximum transport velocity when the beginning of the gliding phase coincides with that of the positive phase of the driving cycle. On the other side, the minimum transport velocity is obtained when the motion of the granular block consists of hopping without gliding.

We can read of Fig. 2 a general decrease of the transport velocity efficiency as the inclination angle α increases. For α = 10°, the figure shows a current reversal with positive (uphill) velocity efficiency around the two transport maximums. For the same inclination angle and a higher friction coefficient (μ = 0.6), the velocity efficiency is positive only around the second maximum at Γ = 4.7. As we further increase the inclination angle, the decrease of the transport velocity efficiency becomes larger leading to the suppression of the positive (uphill) transport flow in the investigated throw number range ($0 \leq \Gamma \leq 6$) at α = 30°, and subsequently, the suppression of the current reversal.

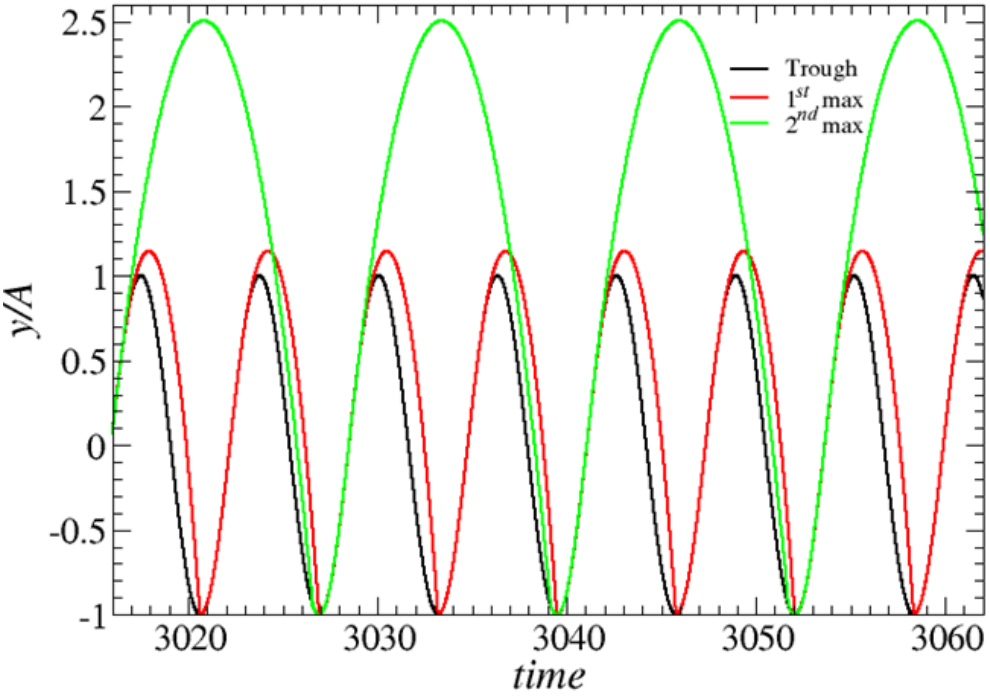

FIG. 5: The vertical motion of the table (black solid line) and of the granular block at the first maximum Γ=1.7 (re solid lined) and the second maximum Γ=4.8 (green solid line) as function of time, calculated using a solid friction coefficient μ = 0.3.

To investigate the dependence of the current reversal on the inclination angle, we calculate the velocity efficiency η for different inclination angles α, while we fix all the other parameters including the throw number Γ. We set the throw number to Γ = 4.7 which corresponds to the largest transport velocity efficiency in the investigated throw numbers range. We calculate the velocity efficiency η for inclination angle α in the range $0 \leq \alpha \leq 40°$ with an angle step $\Delta\alpha = 1°$. For comparison, we use two different friction coefficients μ = 0.3 and μ = 0.6 as well as three different tangential restitution coefficients ε_t = 0.2, 0.7 and 0.9.

We can read off Fig. 6, which shows the results of these calculations, the decrease of the transport velocity efficiency as the inclination angle increases. This decrease is due to the increase of the magnitude of the tangential component of the gravitational force. The figure shows that this decrease is faster with the larger tangential restitution coefficient, $\varepsilon_t = 0.9$ and the smaller friction coefficient, μ = 0.3. This stems from the facts that, first, as the dynamics of the granular block in a free flight phase are mainly driven by the gravitational force, the motion of the block is mainly downhill with negative impact velocity. A larger tangential restitution coefficient promotes a downhill flow by conserving this impact negative velocity. This effect increase as the inclination angle increases leading to a faster decrease of the transport velocity efficiency with increasing inclination angle. Second, the friction force resists the flow leading to a decrease of the magnitude of the transport velocity in both directions, and hence leads to a slower rate of change of the transport velocity efficiency as function of the inclination angle α. The figure also shows the existence of a limit inclination angle $\alpha_0(\mu, \varepsilon_t)$ above which the transport velocity efficiency is negative. This inclination angle depends on the friction coefficient μ and the tangential restitution coefficient ε_t. We find that $\alpha_0(0.3, 0.9) \approx 14°$, $\alpha_0(0.3, 0.7) \approx 18°$, $\alpha_0(0.6, 0.7) \approx 22°$ and finally $\alpha_0(0.3, 0.2) \approx 30°$. Since the velocity efficiency is maximal at Γ = 4.7, we assume that above $\alpha_0(\mu, \varepsilon_t)$, the transport velocity efficiency is negative all over the range of throw numbers $0 \leq \Gamma \leq 6.0$, meaning a suppression of the current reversal.

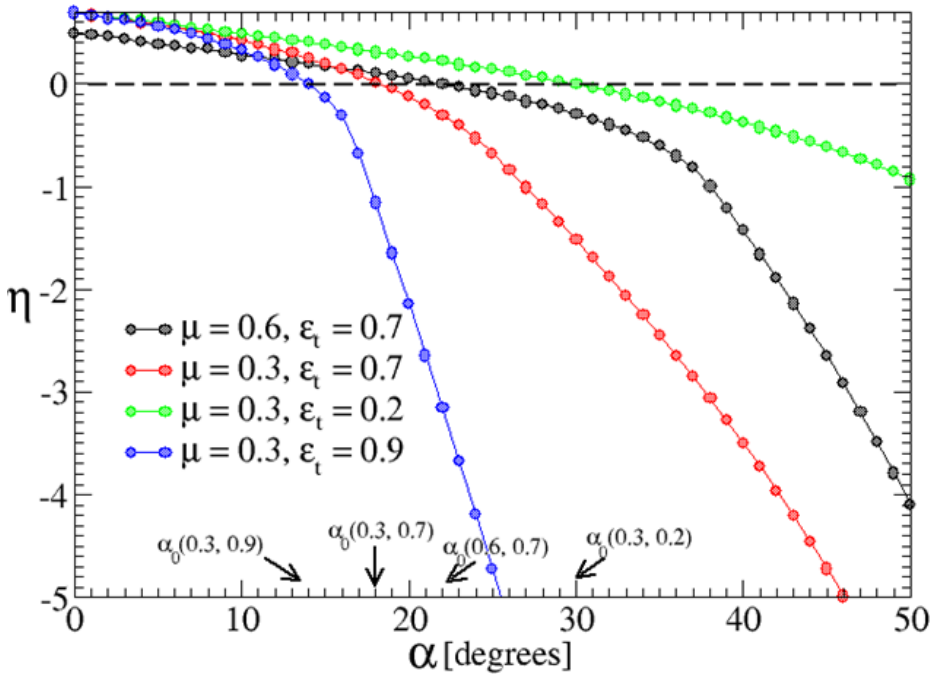

FIG.6: The transport velocity efficiency η as function of the inclination angle α calculated for Γ=4.7, ε_t = 0.7 and for two different friction coefficients μ = 0.3 and 0.6.

IV. CONCLUSION

I have presented a model for the determination of transport velocity efficiency of granular materials on an inclined vibratory conveyor subject to a circular driving mode. My calculations show the persistence, under certain conditions of the major features of the transport found for a horizontal conveyor, in particular the current reversal and the optimal transport condition. Based on this model, we could explain the origin of the different behavior of the transport velocity and the underlying dynamics. The calculations show the existence of a new transport minimum due to the competition between the gravitational and the driving forces. This minimum is strongly friction dependent. The calculations also show that by increasing the inclination angle we obtain a suppression of the current reversal. This suppression does depend on the elastic as well as the friction properties of the granular block. Finally, I hope that experimental studies will be performed in the future to validate the model predictions.

V. REFERENCES

[1] W. H. Hsieh and C. H. Tsai, A study on a novel vibrating conveyor, Key Eng Mater; 419: 4548 (2010).

[2] M. O. Hongler, P. Cartier and P. Flury, Numerical study of a model of vibro-transporter, Phys. Lett. A 135 106 (1989).

[3] F. J. C. Rademacher and L. ter Borg, On the theoretical and experimental conveying speed of granular bulk solids on vibratory conveyors, Eng. Res. 60 261 (1994).

[4] F. J. C. Rademacher, On the theoretical and experimental conveying speed of granular bulk solids on vibratory conveyors, Bulk Solids Handling 15(1) 41 (1995).

[5] K. Erdesz and J. Nemeth, Methods of calculation of vibrational transport rate of granular materials, Powder Tech. 55(3), 161170 (1988).

[6] K. Erdesz and A. Szalay, Experimental study on the vibrational transport of bulk solids, Powder Tech. 55(2), 8796 (1988).

[7] G. H. L. Harding and R. M. Nedderman, The flight-free vibrating conveyor—part 2: stability analysis and criteria for optimal design, Chem. Eng. Res. Des. 68, 131138 (1990).

[8] E. M. Sloot and N. P. Kruyt, Theoretical and experimental study of the transport of granular materials by inclined vibratory conveyors,

Powder Techn. 87(3) 203 (1996).

[9] R. Grochowski, P. Walzel, M. Rouijaa, C. A. Kruelle and I. Rehberg, Reversing granular flow on a vibratory conveyor, Appl. Phys. Lett. 84(6), 1019 (2004).

[10] C. A. Kruelle, M. Rouijaa, A. Goetzendorfer, I. Rehberg, R. Grochowski, P. Walzel, H. El hor and S. J. Linz, Reversal of a granular flow on a vibratory conveyor, Powders and Grains 2005 1185 (2005).

[11] H. El hor and S. J. Linz, Model for transport of granular matter on an annular vibratory conveyor, J. Stat. Mech. L02005, (2005).

[12] H. El hor, S. J. Linz, R. Grochowski, P. Walzel, C. A. Kruelle and I. Rehberg, Model for transport of granular matter on vibratory conveyors, Powders and Grains 1191 (2005).

[13] J. D. Goddard and A. K. Didwania, A fluid-like model of vibrated granular layers: linear stability, kinks, and oscillons, Mech. Mater. 41(6), 637651 (2009).

[14] J. D. Goddard, Frictionless conveying of frictional materials, Granular Matter 14:145149 (2012).

[15] H. W. Ma and G, Fang, Kinematics analysis and experimental investigation of an inclined feeder with horizontal vibration, Proceedings of the IMechE, 230-17, 3147(2016).

[16] J. L. Anthony and C. Marone, Influence of particle characteristics on granular friction, J. Geophys. Res., 110, B08409 (2005).

[17] H. Lastakowski, J. C. Géminard and V. Vidal, Granular friction: Triggering large events with small vibrations, Sci. Rep. 5, 13455 (2015).